

# Study of $\Sigma N$ interaction from the $\Sigma p$ scattering experiment at J-PARC

K. Miwa<sup>1</sup>, J.K. Ahn<sup>2</sup>, Y. Akazawa<sup>3</sup>, T. Aramaki<sup>1</sup>, S. Ashikaga<sup>4</sup>, S. Callier<sup>5</sup>, N. Chiga<sup>1</sup>, S. W. Choi<sup>2</sup>, H. Ekawa<sup>6</sup>, P. Evtoukhovitch<sup>7</sup>, N. Fujioka<sup>1</sup>, M. Fujita<sup>1</sup>, T. Gogami<sup>4</sup>, T. Harada<sup>4</sup>, S. Hasegawa<sup>8</sup>, S.H. Hayakawa<sup>8</sup>, R. Honda<sup>1</sup>, S. Hoshino<sup>9</sup>, K. Hosomi<sup>8</sup>, M. Ichikawa<sup>4</sup>, Y. Ichikawa<sup>8</sup>, M. Ieiri<sup>3</sup>, M. Ikeda<sup>1</sup>, K. Imai<sup>8</sup>, Y. Ishikawa<sup>1</sup>, S. Ishimoto<sup>3</sup>, W. S. Jung<sup>2</sup>, S. Kajikawa<sup>1</sup>, H. Kanauchi<sup>1</sup>, H. Kanda<sup>10</sup>, B. M. Kang<sup>2</sup>, H. Kawai<sup>11</sup>, S. H. Kim<sup>2</sup>, K. Kobayashi<sup>9</sup>, T. Koike<sup>1</sup>, K. Matsuda<sup>1</sup>, Y. Matsumoto<sup>1</sup>, S. Nagao<sup>1</sup>, R. Nagatomi<sup>9</sup>, Y. Nakada<sup>9</sup>, M. Nakagawa<sup>6</sup>, I. Nakamura<sup>3</sup>, T. Nanamura<sup>4,8</sup>, M. Naruki<sup>4</sup>, S. Ozawa<sup>1</sup>, L. Raux<sup>5</sup>, T. Rogers<sup>1</sup>, A. Sakaguchi<sup>9</sup>, T. Sakao<sup>1</sup>, H. Sako<sup>8</sup>, S. Sato<sup>8</sup>, T. Shiozaki<sup>1</sup>, K. Shirotori<sup>10</sup>, K. N. Suzuki<sup>4</sup>, S. Suzuki<sup>3</sup>, M. Tabata<sup>11</sup>, C. d. L. Taille<sup>5,3</sup>, H. Takahashi<sup>3</sup>, T. Takahashi<sup>3</sup>, T. N. Takahashi<sup>10</sup>, H. Tamura<sup>1,8</sup>, M. Tanaka<sup>3</sup>, K. Tanida<sup>8</sup>, Z. Tsamalaidze<sup>7,12</sup>, M. Ukai<sup>3</sup>, H. Umetsu<sup>1</sup>, T. O. Yamamoto<sup>8</sup>, J. Yoshida<sup>8</sup> and K. Yoshimura<sup>13</sup>

<sup>1</sup> Department of Physics, Tohoku University, Japan.

<sup>2</sup> Department of Physics, Korea University, Korea

<sup>3</sup> High Energy Accelerator Research Organization (KEK), Japan

<sup>4</sup> Department of Physics, Kyoto University, Japan

<sup>5</sup> OMEGA Ecole Polytechnique-CNRS/IN2P3, France

<sup>6</sup> RIKEN, Japan

<sup>7</sup> Joint Institute for Nuclear Research (JINR), Dubna, Russia

<sup>8</sup> Japan Atomic Energy Agency (JAEA), Japan

<sup>9</sup> Department of Physics, Osaka University, Japan

<sup>10</sup> Research Center for Nuclear Physics (RCNP), Osaka University, Japan

<sup>11</sup> Department of Physics, Chiba University, Japan

<sup>12</sup> Georgian Technical University (GTU), Tbilisi, Georgia

<sup>13</sup> Department of Physics, Okayama University, Japan

E-mail: miwa9@lambda.phys.tohoku.ac.jp

**Abstract.** A high statistics  $\Sigma p$  scattering experiment has been performed at the K1.8 beamline in the J-PARC Hadron Experimental Facility. Data for momentum-tagged  $\Sigma^-$  beam running in a liquid hydrogen target were accumulated by detecting the  $\pi^- p \rightarrow K^+ \Sigma^-$  reaction with a high intensity  $\pi^-$  beam of 20 M/spill. The number of the  $\Sigma^-$  beam was about  $1.7 \times 10^7$  in total. The  $\Sigma^- p$  elastic scattering and the  $\Sigma^- p \rightarrow \Lambda n$  inelastic scattering events were successfully observed with about 100 times larger statistics than that in past experiments.

## 1. Introduction

Investigation of the baryon-baryon (BB) interaction is one of the most important topics in strangeness nuclear physics. This is because the BB interaction is the basic interaction to describe a system including hyperons such as hypernuclei and a high density nuclear matter in neutron stars. The BB interaction is also a key to understand the origin of the short range core in nuclear force. Historically, the hyperon nucleon (YN) interaction, that is a strangeness  $-1$  sector of the BB interaction, has been investigated experimentally by the spectroscopic studies of hypernuclei with high resolution because their energy levels reflect the spin-dependent YN interaction [1]. Theoretically, the interaction models such as fss2, ESC08 which are based on the quark cluster model (QCM) and boson exchange picture, respectively, have been constructed based on very limited two-body YN scattering data and with the assumption of the flavor SU(3) symmetry [2] [3] [4]. These models were updated and improved to reproduce the experimental data of hypernuclei. The chiral effective field theory has been also applied to the YN and YY interaction and the calculation in the next leading order has been already performed [5]. Nowadays, a lattice QCD simulation is one of the most powerful methods to derive the BB potentials from the first principle in QCD. It also demonstrated a variety of features in the core parts such as strongly repulsive cores due to the Pauli principle between quarks with the same configuration of spin, flavor and color [6] [7] and this quark Pauli effect was originally predicted by QCM. For example, the  ${}^3S_1$  state of the  $\Sigma^+p$  channel is the partially Pauli forbidden channel because a pair of  $up$  quarks in this system has the same spin and color with a large probability. In this situation, it is quite important to give a quantitative information about the size of the large repulsive force due to quark Pauli effect which is included in the  $\Sigma^+p$  channel, experimentally. The systematic studies of the wide flavor configurations are also essential to test the theoretical framework extended to the BB interaction under the flavor SU(3) symmetry.

Hyperon proton scattering experiment is the most direct method to derive the YN interaction as in the case of the nucleon nucleon interaction. However, the hyperon proton scattering experiment is quite difficult due to the short lifetime of hyperons and data of hyperon proton scattering are quite scarce. In order to overcome this experimental difficulty and to investigate the  $\Sigma N$  interaction, we proposed a  $\Sigma p$  scattering experiment (J-PARC E40) to measure differential cross sections of the  $\Sigma^+p, \Sigma^-p$  elastic scatterings and the  $\Sigma^-p \rightarrow \Lambda n$  inelastic scattering in the momentum range of  $400 < p \text{ (MeV/c)} < 700$  [8]. The physics motivation is to verify the large repulsive force due to Pauli effect in the quark level in the  $\Sigma^+p$  channel. The differential cross section of  $\Sigma^+p$  scattering is one of the best observables to reveal the nature of this quark Pauli effect because the magnitude of the repulsive force depends on the cross section at the momentum range. We also investigate the  $\Sigma N$  interaction systematically by separating isospin channels. These are essential data for investigating the spin isospin dependence of the  $\Sigma N$  interaction.

## 2. Experiment at J-PARC

We have performed the first period of the  $\Sigma p$  scattering experiment (J-PARC E40) at the K1.8 beamline in the J-PARC Hadron Experimental Facility. We have introduced a new experimental technique to overcome the experimental difficulty of a hyperon proton scattering experiment due to the hyperon's short lifetime. A liquid hydrogen (LH<sub>2</sub>) target is used as both  $\Sigma$  production and  $\Sigma p$  scattering targets. Because both the  $\Sigma$  production reaction ( $\pi^\pm p \rightarrow K^+ \Sigma^\pm$ ) and the  $\Sigma p$  scattering reaction ( $\Sigma p \rightarrow \Sigma p$ ) are "two-body reactions" as shown in the left part of Figure 1, the  $\Sigma p$  scattering events can be identified kinematically by measuring four-momentum vectors of  $\pi^\pm$  beam,  $K^+$ , and recoil proton. The momentum of the produced  $\Sigma$  particles is obtained from the momenta of  $\pi$  beam particles and scattered  $K^+$  measured by the K1.8 beamline spectrometer and the KURAMA spectrometer, respectively, as shown in Figure 1. In Figure 1, a schematic view of the experimental setup around the target is shown. The LH<sub>2</sub> target is surrounded by

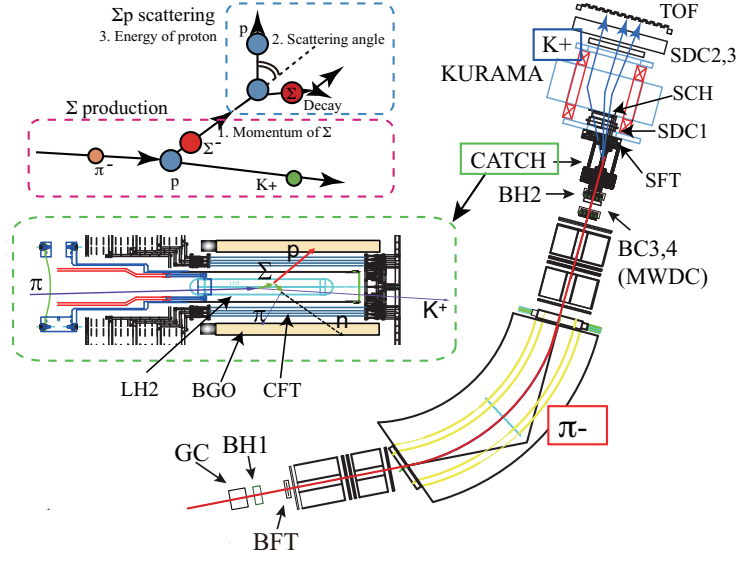


**Figure 1.** Experimental concept of the  $\Sigma p$  scattering experiment and the experimental setup. By using a liquid hydrogen ( $\text{LH}_2$ ) target as both  $\Sigma$  production and  $\Sigma p$  scattering targets, two successive two-body reactions of the  $\Sigma$  production reaction ( $\pi^\pm p \rightarrow K^\pm \Sigma^\pm$ ) and the  $\Sigma p$  scattering reaction ( $\Sigma p \rightarrow \Sigma p$ ) will be measured. The beamline spectrometer consists of two hodoscopes (BH1 and BH2) and three position detectors (BFT, BC3 and BC4). In the KURAMA spectrometer, five position detectors (SFT, SDC1, SCH, SDC2 and SDC3) and a TOF counter are used. The CATCH system consisting of a fiber tracker (CFT) and a BGO calorimeter surrounds the  $\text{LH}_2$  target.

the CATCH (Cylindrical Active Tracker and Calorimeter system for Hyperon-proton scattering) detector system which consists of a cylindrical fiber tracker (CFT) and a BGO calorimeter[9]. The trajectory of the recoil proton is reconstructed by CFT, and the scattering angle of the  $\Sigma p$  scattering can be measured as the crossing angle between the vectors of the  $\Sigma$  beam and recoil proton. The kinetic energy is also measured by the BGO calorimeter and CFT. Then, we check whether the relation of the scattering angle and the kinetic energy is consistent with the  $\Sigma p$  scattering kinematics or not. We also detect charged particles from the  $\Sigma$  decay to suppress the background.

We started the experiment from the  $\Sigma^- p$  channel. This channel is suitable to check the experimental feasibility by detecting proton in coincidence with the  $\Sigma^-$  production because  $\Sigma^-$  mainly decays to  $n\pi^-$  and the detected proton is attributed to secondary reaction of the produced  $\Sigma^-$  particle. The experiment was performed during about 20 days from the middle of February in 2019. In this proceedings, we report the analysis status of the  $\Sigma^- p$  channel.

### 3. Analysis

$\Sigma^-$  particles were identified from the missing mass spectrum of the  $\pi^- p \rightarrow K^+ X$  reaction as shown in Figure 2, where the momenta of the  $\pi^-$  beam and the scattered  $K^+$  were analyzed by the K1.8 beamline spectrometer and the KURAMA spectrometer, respectively. A clear peak corresponding to  $\Sigma^-$  could be identified and background contamination under the  $\Sigma^-$  mass region from  $1.17 \text{ GeV}/c^2$  to  $1.24 \text{ GeV}/c^2$  was about 8%. About  $1.7 \times 10^7$   $\Sigma^-$ 's were accumulated in total and this yield was about 100 times larger yield than that in previous KEK experiment[10]. The momentum of  $\Sigma^-$  was obtained from the missing momentum of the  $\pi^- p \rightarrow K^+ X$  reaction. The  $\Sigma^-$  beam momentum ranged from  $0.45 \text{ GeV}/c$  to  $0.85 \text{ GeV}/c$

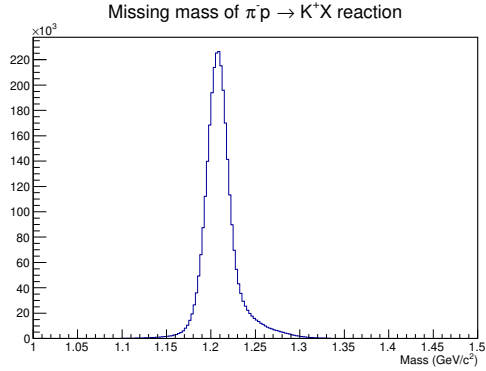


**Figure 2.** Missing mass spectrum of the  $\pi^-p \rightarrow K^+X$  reaction. The  $\Sigma^-$  peak can be clearly identified.

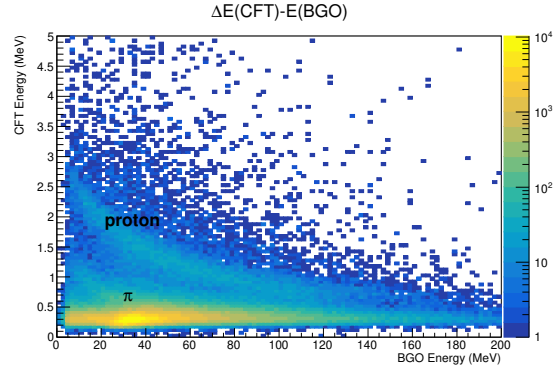


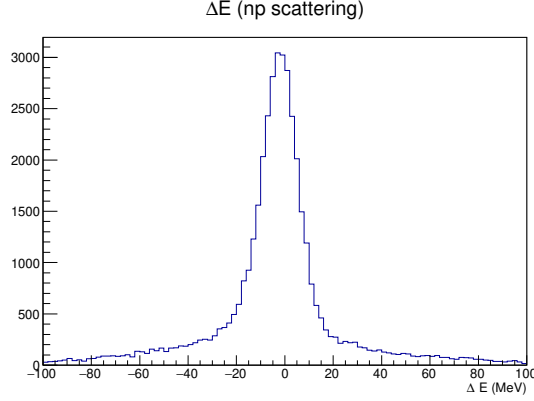
**Figure 3.**  $\Delta E$ - $E$  spectrum between the energy deposit in CFT and the total energy measured by the BGO calorimeter. Locus corresponding proton can be identified.

continuously and this momentum range was determined by the kinematics of the  $\pi^-p \rightarrow K^+\Sigma^-$  reaction and the acceptance of the KURAMA spectrometer. We describe this tagged  $\Sigma^-$  particle as  $\Sigma^-$  beam. In the present analysis, all  $\Sigma^-$  beam events were used without separating its momentum.

The  $\Sigma^-$  beam could be scattered by a proton along its path in the LH<sub>2</sub> target with some probabilities. The recoil proton and the decay  $\pi^-$  from the scattered  $\Sigma^-$  were detected by the CATCH system. Pulse height informations of the BGO calorimeter and CFT were calibrated to energy deposits by using a  $pp$  scattering data with 0.6 and 0.65 GeV/ $c$  proton beams. The particle identification in CATCH was performed by so called  $\Delta E$ - $E$  method between the energy deposit in CFT ( $\Delta E$ ) and the total energy deposit in BGO ( $E$ ). Figure 3 shows the  $\Delta E$ - $E$  plot when the  $\Sigma^-$  events were selected from the missing mass spectrum of the  $\pi^-p \rightarrow K^+X$  reaction. The locus corresponding to proton could be identified and this meant that there was a secondary reaction originating in the  $\Sigma^-$  particle. Some of these proton events might originate in the  $\Sigma^-p$  scattering or the  $\Sigma^-p \rightarrow \Lambda n$  scattering. However, many of these protons came from the scattering of the decay product from  $\Sigma^-$  such as  $np$  and  $\pi^-p$  scatterings after the  $\Sigma^- \rightarrow n\pi^-$  decay. Such events were background events for the  $\Sigma^-p$  scattering. However, these events could be used to check the experimental performance by reconstructing the  $np$  scattering events.

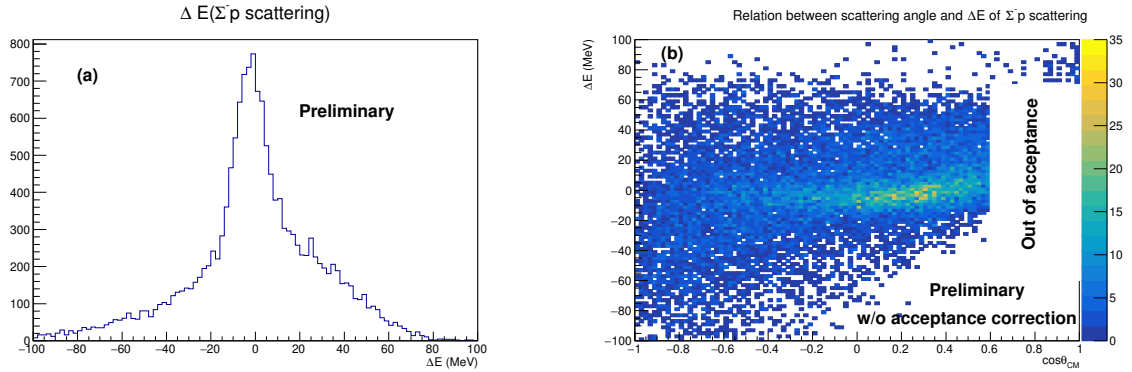
Here, we explain how the scattering events can be identified through the example of the  $np$  scattering from the  $\Sigma^-$  decay. The momentum vector of the  $\Sigma^-$  beam is reconstructed from the spectrometer informations. The neutron momentum from  $\Sigma^-$  can be calculated from the  $\pi^-$  information detected by CATCH assuming that  $\pi^-$  was emitted from the  $\Sigma^-$  decay. Then, we assume that the neutron was scattered by proton and the recoil proton was detected by CATCH. The proton energy is measured by the BGO calorimeter and the measured energy is described as  $E_{measured}$  here. On the other hand, the proton's energy can be calculated from the scattering angle of the proton with an assumption of the  $np$  scattering. Here, the calculated energy is described as  $E_{calculated}$ . Then we define the  $\Delta E$  as the difference between  $E_{measured}$  and  $E_{calculated}$  ( $\Delta E = E_{measured} - E_{calculated}$ ). If the recoil proton really originated in the  $np$  scattering, such events would make a peak around  $\Delta E = 0$  in the  $\Delta E$  spectrum. Figure 4 shows the  $\Delta E$  spectrum with the assumption of the  $np$  scattering. A clear peak corresponding to the  $np$  scattering can be identified at  $\Delta E = 0$ . In this way, other  $\Delta E$  spectra ( or  $\Delta p$  spectra) can be made by changing the assumption of the reaction kinematics.

Figure 5 (a) and Figure 6 (a) show the  $\Delta E$  and  $\Delta p$  spectra assuming that the reactions are the



**Figure 4.**  $\Delta E$  spectrum assuming the  $np$  elastic scattering. The peak corresponding to the  $np$  elastic scattering can be identified at  $\Delta E = 0$  above the background structure.

$\Sigma^-p$  elastic scattering and the  $\Sigma^-p \rightarrow \Lambda n$  scattering, respectively. Clear peaks corresponding to the  $\Sigma^-p$  elastic scattering and the  $\Sigma^-p \rightarrow \Lambda n$  scattering can be identified at  $\Delta E$  (or  $\Delta p$ ) = 0 above the background structure. About 4,500 and 2,400 of events have been observed for the  $\Sigma^-p$  elastic scattering and the  $\Sigma^-p \rightarrow \Lambda n$  scattering, respectively, from  $1.7 \times 10^7$   $\Sigma^-$  beam. These are about 100 times larger statistics than past experimental results in this momentum region[10]. Figure 5 (b) and Figure 6 (b) show the correlations between the  $\Delta E$  (or  $\Delta p$ ) and  $\cos(\theta_{CM})$  before the acceptance and efficiency correction, where  $\theta_{CM}$  is the scattering angle of hyperon at the center of mass system. Although a part of the angular region is out of acceptance due to the low energy of the recoil proton, much wider angular acceptance has been realized. Now analysis is on going to derive the differential cross sections of these reactions.



**Figure 5.** (a)  $\Delta E$  spectrum assuming the  $\Sigma^-p$  elastic scattering. The peak corresponding to the  $\Sigma^-p$  elastic scattering can be identified at  $\Delta E = 0$  above the background structure. (b) Scatter plot between  $\Delta E$  and  $\cos \theta_{CM}$ , where  $\theta_{CM}$  is the scattering angle of  $\Sigma^-$  in the center of mass system. The acceptance correction is not performed yet. Locus corresponding to the  $\Sigma^-p$  elastic scattering can be identified at  $\Delta E = 0$ .

#### 4. Summary and Prospect

The YN interaction should be investigated directly from the scattering experiment which allows for access to the information without any uncertainty. The  $\Sigma p$  scattering experiment has been

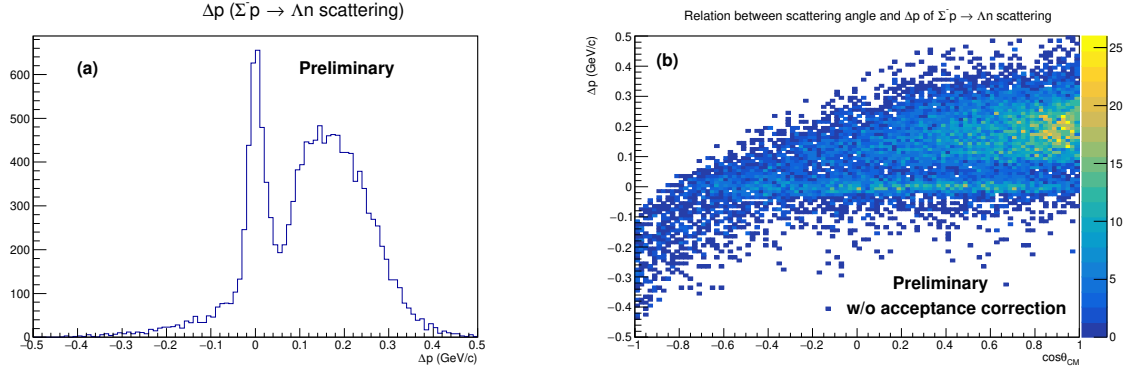


**Figure 6.** (a)  $\Delta p$  spectrum assuming the  $\Sigma^-p \rightarrow \Lambda n$  scattering. The peak corresponding to the  $\Sigma^-p \rightarrow \Lambda n$  scattering can be identified at  $\Delta p = 0$  above the background structure. (b) Scatter plot between  $\Delta p$  and  $\cos\theta_{CM}$ , where  $\theta_{CM}$  is the scattering angle of  $\Lambda$  in the center of mass system. The acceptance correction is not performed yet. Locus corresponding to the  $\Sigma^-p \rightarrow \Lambda n$  scattering can be identified at  $\Delta p = 0$ .

performed at J-PARC in 2019 Spring. In total, about  $1.7 \times 10^7$   $\Sigma^-$  beam was accumulated by using a 20 M/spill  $\pi^-$  beam. The momentum of  $\Sigma^-$  beam ranged from 0.45 to 0.85 GeV/c. The CATCH system, which is a dedicated system to detect a recoil proton from the  $\Sigma p$  scattering, operated stably under high counting rate. We successfully observed about 4,500 events of the  $\Sigma^-p$  elastic scattering and about 2,400 events of the  $\Sigma^-p \rightarrow \Lambda n$  scattering. These statistics are about 100 times larger than that in the past KEK experiment in this momentum range. Data for the  $\Sigma^+p$  elastic scattering were also collected. Analysis to derive the differential cross sections is on going for these three scattering channels.

## 5. Acknowledgement

We would like to express our thanks to the staffs of J-PARC for their support to provide beam during the beam time. They recovered the beam condition many times even after a magnet trouble in the accelerator. We performed a lot of test experiments at accelerator facilities in Tohoku university (CYRIC and ELPH). We would also like to express our thanks to the staffs of CYRIC and ELPH for their support to provide beam with the excellent condition during the beam time. This work was supported by JSPS KAKENHI Grant Number 23684011, 15H05442, 15H02079 and 18H03693. This work was also supported by Grants-in-Aid Number 24105003 and 18H05403 for Scientific Research from the Ministry of Education, Culture, Science and Technology (MEXT) Japan.

## References

- [1] O. Hashimoto and H. Tamura, Prog. Part. Nucl. Phys. **57**,564 (2006).
- [2] M. Oka and K. Shimizu and K. Yazaki, Nucl. Phys. A**464**, 700 (1987).
- [3] C. Nakamoto, Y. Suzuki and Y. Fujiwara, Prog. Theor. Phys. **94**, 65 (1995).
- [4] T.A. Rijken, M.M. Nagels and Y. Yamamoto, Prog. Theor. Phys. Suppl. **185**, 14 (2010).
- [5] J. Haidenbauer, S. Petschauer N. Kaiser, U.-G. Meibner, A. Nogga and W. Weise, Nucl. Phys. A **915**, 24 (2013).
- [6] T. Inoue *et al.* Nucl. Phys. A**881**, 28 (2012).
- [7] H. Nemura *et al.* AIP Conf. Proc. **2130**, 040005 (2019).
- [8] K. Miwa *et al.* JPS Conf. Proc. **17**,012004 (2017).
- [9] Y. Akazawa, Doctor thesis, Tohoku university (2018).
- [10] Y. Kondo *et al.* Nucl. Phys. A **676**,371 (2000).